

Dijet Production by Color-Singlet Exchange at the Fermilab Tevatron

- F. Abe,¹⁷ H. Akimoto,³⁸ A. Akopian,³¹ M. G. Albrow,⁷ S. R. Amendolia,²⁷ D. Amidei,²⁰ J. Antos,³³ S. Aota,³⁶
 G. Apollinari,³¹ T. Arisawa,³⁸ T. Asakawa,³⁶ W. Ashmanskas,¹⁸ M. Atac,⁷ F. Azfar,²⁶ P. Azzi-Bacchetta,²⁵
 N. Bacchetta,²⁵ W. Badgett,²⁰ S. Bagdasarov,³¹ M. W. Bailey,²² J. Bao,⁴⁰ P. de Barbaro,³⁰ A. Barbaro-Galtieri,¹⁸
 V. E. Barnes,²⁹ B. A. Barnett,¹⁵ M. Barone,⁹ E. Barzi,⁹ G. Bauer,¹⁹ T. Baumann,¹¹ F. Bedeschi,²⁷ S. Behrends,³
 S. Belforte,²⁷ G. Bellettini,²⁷ J. Bellinger,³⁹ D. Benjamin,³⁵ J. Benlloch,¹⁹ J. Bensinger,³ D. Benton,²⁶ A. Beretvas,⁷
 J. P. Berge,⁷ J. Berryhill,⁵ S. Bertolucci,⁹ S. Bettelli,²⁷ B. Bevensee,²⁶ A. Bhatti,³¹ K. Biery,⁷ M. Binkley,⁷ D. Bisello,²⁵
 R. E. Blair,¹ C. Blocker,³ S. Blusk,³⁰ A. Bodek,³⁰ W. Bokhari,²⁶ G. Bolla,²⁹ V. Bolognesi,² Y. Bonushkin,⁴
 D. Bortoletto,²⁹ J. Boudreau,²⁸ L. Breccia,² C. Bromberg,²¹ N. Bruner,²² E. Buckley-Geer,⁷ H. S. Budd,³⁰ K. Burkett,²⁰
 G. Busetto,²⁵ A. Byon-Wagner,⁷ K. L. Byrum,¹ C. Campagnari,⁷ M. Campbell,²⁰ A. Caner,²⁷ W. Carithers,¹⁸
 D. Carlsmith,³⁹ J. Cassada,³⁰ A. Castro,²⁵ D. Cauz,²⁷ Y. Cen,³⁰ A. Cerri,²⁷ F. Cervelli,²⁷ P. S. Chang,³³ P. T. Chang,³³
 H. Y. Chao,³³ J. Chapman,²⁰ M.-T. Cheng,³³ M. Chertok,³⁴ G. Chiarelli,²⁷ T. Chikamatsu,³⁶ C. N. Chiou,³³
 L. Christofek,¹³ S. Cihangir,⁷ A. G. Clark,¹⁰ M. Cobal,²⁷ E. Cocca,²⁷ M. Contreras,⁵ J. Conway,³² J. Cooper,⁷
 M. Cordelli,⁹ C. Couyoumtzelis,¹⁰ D. Crane,¹ D. Cronin-Hennessy,⁶ R. Culbertson,⁵ T. Daniels,¹⁹ F. DeJongh,⁷
 S. Delchamps,⁷ S. Dell'Agnello,²⁷ M. Dell'Orso,²⁷ R. Demina,⁷ L. Demortier,³¹ M. Deninno,² P. F. Derwent,⁷
 T. Devlin,³² J. R. Dittmann,⁶ S. Donati,²⁷ J. Done,³⁴ T. Dorigo,²⁵ A. Dunn,²⁰ N. Eddy,²⁰ K. Einsweiler,¹⁸ J. E. Elias,⁷
 R. Ely,¹⁸ E. Engels, Jr.,²⁸ D. Errede,¹³ S. Errede,¹³ Q. Fan,³⁰ G. Feild,⁴⁰ Z. Feng,¹⁵ C. Ferretti,²⁷ I. Fiori,² B. Flaugher,⁷
 G. W. Foster,⁷ M. Franklin,¹¹ M. Frautschi,³⁵ J. Freeman,⁷ J. Friedman,¹⁹ H. Frisch,⁵ Y. Fukui,¹⁷ S. Funaki,³⁶
 S. Galeotti,²⁷ M. Gallinaro,³⁵ O. Ganel,³⁵ M. Garcia-Sciveres,¹⁸ A. F. Garfinkel,²⁹ C. Gay,¹¹ S. Geer,⁷ D. W. Gerdes,¹⁵
 P. Giannetti,²⁷ N. Giokaris,³¹ G. Giusti,²⁷ L. Gladney,²⁶ M. Gold,²² J. Gonzalez,²⁶ A. Gordon,¹¹ A. T. Goshaw,⁶
 Y. Gotra,²⁵ K. Goulianos,³¹ H. Grassmann,²⁷ L. Groer,³² C. Grossi-Pilcher,⁵ G. Guillian,²⁰ J. Guimaraes,¹⁵
 R. S. Guo,³³ C. Haber,¹⁸ E. Hafen,¹⁹ S. R. Hahn,⁷ R. Hamilton,¹¹ R. Handler,³⁹ R. M. Hans,⁴⁰ F. Happacher,⁹
 K. Hara,³⁶ A. D. Hardman,²⁹ B. Harral,²⁶ R. M. Harris,⁷ S. A. Hauger,⁶ J. Hauser,⁴ C. Hawk,³² E. Hayashi,³⁶
 J. Heinrich,²⁶ B. Hinrichsen,¹⁴ K. D. Hoffman,²⁹ M. Hohlmann,⁵ C. Holck,²⁶ R. Hollebeek,²⁶ L. Holloway,¹³
 S. Hong,²⁰ G. Houk,²⁶ P. Hu,²⁸ B. T. Huffman,²⁸ R. Hughes,²³ J. Huston,²¹ J. Huth,¹¹ J. Hylen,⁷ H. Ikeda,³⁶
 M. Incagli,²⁷ J. Incandela,⁷ G. Introzzi,²⁷ J. Iwai,³⁸ Y. Iwata,¹² H. Jensen,⁷ U. Joshi,⁷ R. W. Kadel,¹⁸ E. Kajfasz,²⁵
 H. Kambara,¹⁰ T. Kamon,³⁴ T. Kaneko,³⁶ K. Karr,³⁷ H. Kasha,⁴⁰ Y. Kato,²⁴ T. A. Keaffaber,²⁹ K. Kelley,¹⁹
 R. D. Kennedy,⁷ R. Kephart,⁷ P. Kesten,¹⁸ D. Kestenbaum,¹¹ H. Keutelian,⁷ F. Keyvan,⁴ B. Kharadja,¹³ B. J. Kim,³⁰
 D. H. Kim,^{7,*} H. S. Kim,¹⁴ S. B. Kim,²⁰ S. H. Kim,³⁶ Y. K. Kim,¹⁸ L. Kirsch,³ P. Koehn,²³ A. Konigeter,¹⁶ K. Kondo,³⁶
 J. Konigsberg,⁸ S. Kopp,⁵ K. Kordas,¹⁴ A. Korytov,⁸ W. Koska,⁷ E. Kovacs,^{7,*} W. Kowald,⁶ M. Krasberg,²⁰ J. Kroll,⁷
 M. Kruse,³⁰ S. E. Kuhlmann,¹ E. Kuns,³² T. Kuwabara,³⁶ A. T. Laasanen,²⁹ S. Lami,²⁷ S. Lammel,⁷ J. I. Lamoureux,³
 M. Lancaster,¹⁸ M. Lanzoni,²⁷ G. Latino,²⁷ T. LeCompte,¹ S. Leone,²⁷ J. D. Lewis,⁷ P. Limon,⁷ M. Lindgren,⁴
 T. M. Liss,¹³ J. B. Liu,³⁰ Y. C. Liu,³³ N. Lockyer,²⁶ O. Long,²⁶ C. Loomis,³² M. Loretta,²⁵ J. Lu,³⁴ D. Lucchesi,²⁷
 P. Lukens,⁷ S. Lusin,³⁹ J. Lys,¹⁸ K. Maeshima,⁷ A. Maghakian,³¹ P. Maksimovic,¹⁹ M. Mangano,²⁷ M. Mariotti,²⁵
 J. P. Marriner,⁷ A. Martin,⁴⁰ J. A. J. Matthews,²² R. Mattingly,¹⁹ P. Mazzanti,² P. McIntyre,³⁴ P. Melese,³¹
 A. Menzione,²⁷ E. Meschi,²⁷ C. Mesropian,³¹ S. Metzler,²⁶ C. Miao,²⁰ T. Miao,⁷ G. Michail,¹¹ R. Miller,²¹ H. Minato,³⁶
 S. Miscetti,⁹ M. Mishina,¹⁷ H. Mitsushio,³⁶ T. Miyamoto,³⁶ S. Miyashita,³⁶ N. Moggi,²⁷ Y. Morita,¹⁷ A. Mukherjee,⁷
 T. Muller,¹⁶ P. Murat,²⁷ S. Murgia,²¹ H. Nakada,³⁶ I. Nakano,³⁶ C. Nelson,⁷ D. Neuberger,¹⁶ C. Newman-Holmes,⁷
 C.-Y. P. Ngan,¹⁹ M. Ninomiya,³⁶ L. Nodulman,¹ S. H. Oh,⁶ K. E. Ohl,⁴⁰ T. Ohmoto,¹² T. Ohsugi,¹² R. Oishi,³⁶
 M. Okabe,³⁶ T. Okusawa,²⁴ R. Oliveira,²⁶ J. Olsen,³⁹ C. Pagliarone,²⁷ R. Paoletti,²⁷ V. Papadimitriou,³⁵ S. P. Pappas,⁴⁰
 N. Parashar,²⁷ S. Park,⁷ A. Parri,⁹ J. Patrick,⁷ G. Paulette,²⁷ M. Paulini,¹⁸ A. Perazzo,²⁷ L. Pescara,²⁵ M. D. Peters,¹⁸
 T. J. Phillips,⁶ G. Piacentino,²⁷ M. Pillai,³⁰ K. T. Pitts,⁷ R. Plunkett,⁷ L. Pondrom,³⁹ J. Proudfoot,¹ F. Ptchos,¹¹
 G. Punzi,²⁷ K. Ragan,¹⁴ D. Reher,¹⁸ A. Ribon,²⁵ F. Rimondi,² L. Ristori,²⁷ W. J. Robertson,⁶ T. Rodrigo,²⁷ S. Rolli,³⁷
 J. Romano,⁵ L. Rosenson,¹⁹ R. Roser,¹³ T. Saab,¹⁴ W. K. Sakumoto,³⁰ D. Saltzberg,⁴ A. Sansoni,⁹ L. Santi,²⁷
 H. Sato,³⁶ P. Schlabbach,⁷ E. E. Schmidt,⁷ M. P. Schmidt,⁴⁰ A. Scott,⁴ A. Scribano,²⁷ S. Segler,⁷ S. Seidel,²² Y. Seiya,³⁶
 F. Semeria,² G. Sganos,¹⁴ T. Shah,¹⁹ M. D. Shapiro,¹⁸ N. M. Shaw,²⁹ Q. Shen,²⁹ P. F. Shepard,²⁸ M. Shimojima,³⁶
 M. Shochet,⁵ J. Siegrist,¹⁸ A. Sill,³⁵ P. Sinervo,¹⁴ P. Singh,¹³ K. Sliwa,³⁷ C. Smith,¹⁵ F. D. Snider,¹⁵ T. Song,²⁰
 J. Spalding,⁷ T. Speer,¹⁰ P. Sphicas,¹⁹ F. Spinella,²⁷ M. Spiropulu,¹¹ L. Spiegel,⁷ L. Stanco,²⁵ J. Steele,³⁹
 A. Stefanini,²⁷ J. Strait,⁷ R. Ströhmer,^{7,*} D. Stuart,⁷ G. Sullivan,⁵ K. Sumorok,¹⁹ J. Suzuki,³⁶ T. Takada,³⁶

T. Takahashi,²⁴ T. Takano,³⁶ K. Takikawa,³⁶ N. Tamura,¹² B. Tannenbaum,²² F. Tartarelli,²⁷ W. Taylor,¹⁴
 P. K. Teng,³³ Y. Teramoto,²⁴ S. Tether,¹⁹ D. Theriot,⁷ T. L. Thomas,²² R. Thun,²⁰ R. Thurman-Keup,¹ M. Timko,³⁷
 P. Tipton,³⁰ A. Titov,³¹ S. Tkaczyk,⁷ D. Toback,⁵ K. Tollefson,³⁰ A. Tollestrup,⁷ H. Toyoda,²⁴ W. Trischuk,¹⁴
 J. F. de Troconiz,¹¹ S. Truitt,²⁰ J. Tseng,¹⁹ N. Turini,²⁷ T. Uchida,³⁶ N. Uemura,³⁶ F. Ukegawa,²⁶ G. Unal,²⁶ J. Valls,^{7,*}
 S. C. van den Brink,²⁸ S. Vejcik III,²⁰ G. Velev,²⁷ R. Vidal,⁷ R. Vilar,^{7,*} M. Vondracek,¹³ D. Vucinic,¹⁹
 R. G. Wagner,¹ R. L. Wagner,⁷ J. Wahl,⁵ N. B. Wallace,²⁷ A. M. Walsh,³² C. Wang,⁶ C. H. Wang,³³ J. Wang,⁵
 M. J. Wang,³³ Q. F. Wang,³¹ A. Warburton,¹⁴ T. Watts,³² R. Webb,³⁴ C. Wei,⁶ H. Wei,³⁵ H. Wenzel,¹⁶
 W. C. Wester III,⁷ A. B. Wicklund,¹ E. Wicklund,⁷ R. Wilkinson,²⁶ H. H. Williams,²⁶ P. Wilson,⁵ B. L. Winer,²³
 D. Winn,²⁰ D. Wolinski,²⁰ J. Wolinski,²¹ S. Worm,²² X. Wu,¹⁰ J. Wyss,²⁵ A. Yagil,⁷ W. Yao,¹⁸ K. Yasuoka,³⁶ Y. Ye,¹⁴
 G. P. Yeh,⁷ P. Yeh,³³ M. Yin,⁶ J. Yoh,⁷ C. Yosef,²¹ T. Yoshida,²⁴ D. Yovanovitch,⁷ I. Yu,⁷ L. Yu,²² J. C. Yun,⁷
 A. Zanetti,²⁷ F. Zetti,²⁷ L. Zhang,³⁹ W. Zhang,²⁶ and S. Zucchelli²

(CDF Collaboration)

¹Argonne National Laboratory, Argonne, Illinois 60439

²Istituto Nazionale di Fisica Nucleare, University of Bologna, I-40127 Bologna, Italy

³Brandeis University, Waltham, Massachusetts 02254

⁴University of California at Los Angeles, Los Angeles, California 90024

⁵University of Chicago, Chicago, Illinois 60637

⁶Duke University, Durham, North Carolina 27708

⁷Fermi National Accelerator Laboratory, Batavia, Illinois 60510

⁸University of Florida, Gainesville, Florida 32611

⁹Laboratori Nazionali di Frascati, Istituto Nazionale di Fisica Nuclear, I-00044 Frascati, Italy

¹⁰University of Geneva, CH-1211 Geneva 4, Switzerland

¹¹Harvard University, Cambridge, Massachusetts 02138

¹²Hiroshima University, Higashi-Hiroshima 724, Japan

¹³University of Illinois, Urbana, Illinois 61801

¹⁴Institute of Particle Physics, McGill University, Montreal H3A 2T8, Canada

and University of Toronto, Toronto M5S 1A7, Canada

¹⁵The Johns Hopkins University, Baltimore, Maryland 21218

¹⁶Institut für Experimentelle Kernphysik, Universität Karlsruhe, 76128 Karlsruhe, Germany

¹⁷National Laboratory for High Energy Physics (KEK), Tsukuba, Ibaraki 315, Japan

¹⁸Ernest Orlando Lawrence Berkeley National Laboratory, Berkeley, California 94720

¹⁹Massachusetts Institute of Technology, Cambridge, Massachusetts 02139

²⁰University of Michigan, Ann Arbor, Michigan 48109

²¹Michigan State University, East Lansing, Michigan 48824

²²University of New Mexico, Albuquerque, New Mexico 87131

²³The Ohio State University, Columbus, Ohio 43210

²⁴Osaka City University, Osaka 588, Japan

²⁵Università di Padova, Istituto Nazionale di Fisica Nucleare, Sezione di Padova, I-36132 Padova, Italy

²⁶University of Pennsylvania, Philadelphia, Pennsylvania 19104

²⁷Istituto Nazionale di Fisica Nucleare, University and Scuola Normale Superiore of Pisa, I-56100 Pisa, Italy

²⁸University of Pittsburgh, Pittsburgh, Pennsylvania 15260

²⁹Purdue University, West Lafayette, Indiana 47907

³⁰University of Rochester, Rochester, New York 14627

³¹Rockefeller University, New York, New York 10021

³²Rutgers University, Piscataway, New Jersey 08855

³³Academia Sinica, Taipei, Taiwan 11530, Republic of China

³⁴Texas A&M University, College Station, Texas 77843

³⁵Texas Tech University, Lubbock, Texas 79409

³⁶University of Tsukuba, Tsukuba, Ibaraki 315, Japan

³⁷Tufts University, Medford, Massachusetts 02155

³⁸Waseda University, Tokyo 169, Japan

³⁹University of Wisconsin, Madison, Wisconsin 53706

⁴⁰Yale University, New Haven, Connecticut 06520

(Received 11 August 1997)

We report a new measurement of dijet production by color-singlet exchange in $p\bar{p}$ collisions at $\sqrt{s} = 1.8$ TeV at the Fermilab Tevatron. In a sample of events with two jets of transverse energy $E_T^{\text{jet}} > 20$ GeV, pseudorapidity in the range $1.8 < |\eta^{\text{jet}}| < 3.5$, and $\eta_1 \eta_2 < 0$, we find that a fraction $R = [1.13 \pm 0.12(\text{stat}) \pm 0.11(\text{syst})]\%$ has a pseudorapidity gap within $|\eta| < 1$ between the jets that

can be attributed to color-singlet exchange. The fraction R shows no significant dependence on E_T^{jet} or on the pseudorapidity separation between the jets. [S0031-9007(97)05184-3]

PACS numbers: 13.87.Fh, 12.38.Qk, 13.85.Hd

In high energy hadron collisions jets are usually produced through the exchange of a quark or gluon between partons of the interacting hadrons. Because of the net color flow associated with such an exchange, particles are commonly produced in the rapidity [1] region between the jets. However, jets may also be produced by a colorless exchange, such as strongly interacting color-singlet or electroweak boson (γ , W , Z^0) exchange, resulting in events with a “rapidity gap” between the jets, namely, a region of rapidity devoid of particles. In a simple model of a two-gluon color-singlet exchange, the ratio of two-jet (dijet) events with a rapidity gap to all two-jet events produced in $p\bar{p}$ collisions at $\sqrt{s} = 1.8$ TeV was estimated to be $R \sim 10^{-2}$ [2,3] independent of rapidity gap width or jet transverse energy (E_T^{jet}); for electroweak exchange, R is expected to be $\sim 10^{-4}$ [3]. The production rate and characteristics of dijet events with a rapidity gap between jets can be used to probe the nature of the colorless exchange process.

The ratio R has been measured in $p\bar{p}$ collisions at $\sqrt{s} = 1.8$ TeV by the CDF [4] and D0 [5] Collaborations at the Fermilab Tevatron, and in photoproduction at a center of mass energy of ~ 150 GeV by the ZEUS Collaboration [6] at HERA. The reported values are $R_{\text{CDF}} = [0.85 \pm 0.12(\text{stat})^{+0.24}_{-0.12}(\text{syst})]\%$ for dijets with leading (highest E_T) jet $E_T > 40$ GeV and $|\Delta\eta| > 1.5$, $R_{\text{D0}} = [1.07 \pm 0.10(\text{stat})^{+0.25}_{-0.13}(\text{syst})]\%$ for $E_T^{\text{jet}} > 30$ GeV, $|\eta^{\text{jet}}| > 2$ and $\eta_1\eta_2 < 0$, and $R_{\text{ZEUS}} \approx 7\%$ for jets of $E_T > 6$ GeV photoproduced at HERA. The magnitude of the measured ratio suggests that the dijet system is produced through strongly interacting color-singlet exchange. In all cases, the background rapidity gap fraction due to normal color-octet exchange was estimated by using Monte Carlo simulations and/or fits to the particle multiplicity distribution in the rapidity region between the jets. In this Letter, we present a new measurement of R at the Tevatron based on a more direct method of background subtraction with different, and smaller, systematic uncertainties. We also present a study of some characteristics of a sample of rapidity gap events, such as third-jet activity and dependence of R on E_T^{jet} and on the rapidity interval between the jets.

The CDF detector is described in detail elsewhere [7]. The detector components relevant to this study are the Central Tracking Chamber (CTC), which detects charged particles, and the calorimeters, which detect both charged and neutral particles. The CTC tracking efficiency varies from $\sim 60\%$ for $P_T = 300$ MeV to over 95% for $P_T > 400$ MeV within $|\eta| < 1.2$, falls monotonically beyond $|\eta| = 1.2$, and approaches zero at $|\eta| \sim 1.8$. The calorimeters have projective tower geometry and cover the regions $|\eta| < 1.1$ (central), $1.1 < |\eta| < 2.4$ (plug),

and $2.2 < |\eta| < 4.2$ (forward). The $\Delta\eta \times \Delta\phi$ tower dimensions are $0.1 \times 15^\circ$ for the central and $0.1 \times 5^\circ$ for the plug and forward calorimeters. For this analysis, a “charged particle” is a reconstructed three-dimensional track with $P_T > 300$ MeV. The “tower multiplicity” is defined as the number of calorimeter towers with measured $E_T > 200$ MeV, which corresponds approximately to true $E_T > 300$ MeV.

The data sample consists of events collected in a run of total integrated luminosity 2.2 pb^{-1} , using a trigger requiring two high E_T jets at $|\eta| > 1.4$. Because of the high instantaneous luminosity during data collection, a large fraction of the events had one or more additional (“minimum bias”) events superimposed on the dijet event that caused the trigger. Since an overlay of minimum bias events could obscure a rapidity gap, we selected a sub-sample of events with no more than one primary reconstructed vertex ($N_{\text{vertex}} \leq 1$) within ± 60 cm of the nominal interaction point. About 16% of the events passed this selection cut. After the jet E_T , defined as the sum of the calorimeter E_T within an $\eta - \phi$ cone of radius 0.7, was corrected for nonlinearities in the calorimeter response and for energy lost in uninstrumented regions, the two leading jets were required to have $E_T^{\text{jet}} > 20$ GeV and $1.8 < |\eta| < 3.5$. No requirement was imposed on additional jets in an event. The remaining dijet sample consists of 10 200 events with the leading jets on opposite η sides ($\eta_1\eta_2 < 0$), and 30 352 events with both leading jets on the same η side ($\eta_1\eta_2 > 0$). The same-side dijet event sample was used for the measurement of the production rate of diffractive dijet events presented in [8]. In this analysis, these events are used in evaluating the color-octet contribution to events with a rapidity gap between jets in the opposite-side sample, as discussed below.

The distributions of the leading jet E_T and η , $E_T^{(1)}$ and η_1 , and of the differences $\Delta E_T = E_T^{(1)} - E_T^{(2)}$ and $\Delta\phi = \phi_1 - \phi_2$ between the two leading jets are shown in Fig. 1. The structure at $|\eta| \sim 2.2-2.4$ is caused by the lower calorimetric response at the interface between different detector components. The two jets tend to be balanced both in E_T and ϕ . About 85% of the events contain a third jet of $E_T^{(3)} > 5$ GeV. The $E_T^{(3)}$ and η_3 distributions of the third jet are also shown in Fig. 1. The corresponding distributions of the same-side dijet sample are very similar [8].

Rapidity gaps between jets can occur naturally in color-octet exchange dijet events by fluctuations of the underlying soft particle multiplicity. We first search for rapidity gaps due to color-singlet exchange by analyzing the event track multiplicity, N_{track} , in the region $|\eta| < 1.0$. Figure 2(a) shows the multiplicity of tracks with

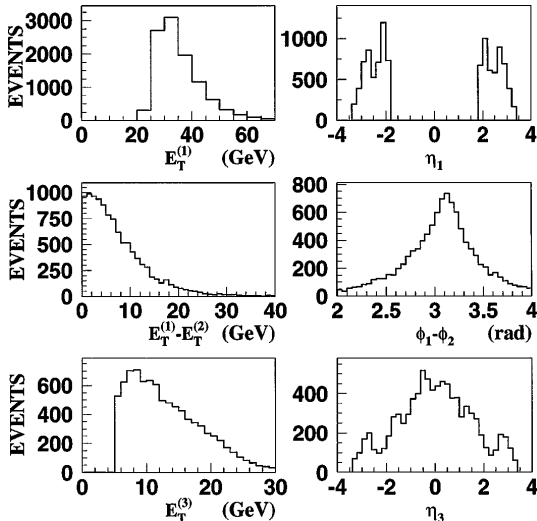


FIG. 1. (top) Leading jet transverse energy and pseudorapidity (the structure at $|\eta| \sim 2.2-2.4$ is instrumental); (middle) difference between the transverse energies and azimuthal angles of the two leading jets; (bottom) third jet ($E_T^{(3)} > 5$ GeV) transverse energy and pseudorapidity.

$P_T > 300$ MeV within $|\eta| < 1.0$ for opposite-side (solid) and within $|\eta| < 1.2$ for same-side (dashed) dijet events. The η range of the same-side distribution was chosen to yield the same mean multiplicity as the opposite-side distribution, and the normalization was scaled down by a factor $C = 0.34$, which is the ratio of opposite-side to same-side events with $N_{\text{track}} > 0$. Figure 2(c) shows the bin-by-bin asymmetry (difference over sum) of the

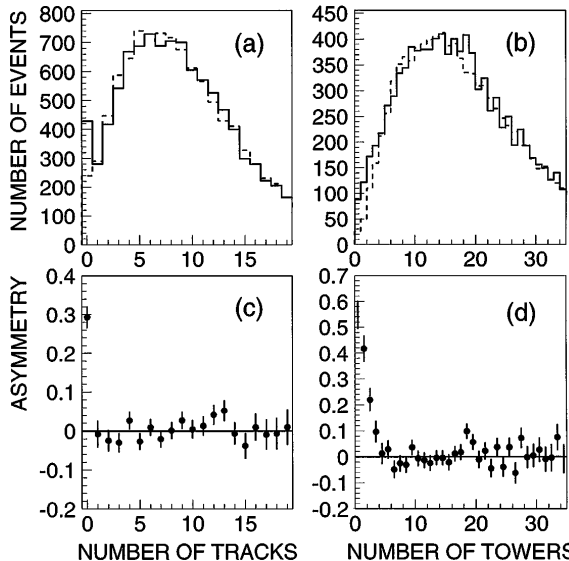


FIG. 2. Multiplicity distributions (a) for tracks with $P_T > 300$ MeV and (b) for calorimeter towers with measured $E_T > 200$ MeV in the regions $|\eta| < 1.0$ for opposite-side ($\eta_1 \eta_2 < 0$) dijet events (solid lines), and $|\eta| < 1.2$ ($|\eta| < 1.25$) for tracks (towers) of same-side ($\eta_1 \eta_2 > 0$) dijet events (dashed lines). (c), (d) The bin-by-bin asymmetry, defined as the ratio of the difference over the sum of the opposite-side and same-side multiplicity distributions of (a) and (b).

two distributions shown in Fig. 2(a). The asymmetry is close to zero in all bins except in the zero-multiplicity bin. From a detailed analysis of the same-side data sample [8], we estimate that the contribution from single diffractive events in the $N_{\text{track}} = 0$ bin of the same-side sample is negligibly small. Thus, the number of events in the $N_{\text{track}} = 0$ bin of the same-side distribution represents approximately the expectation for the number of opposite-side events due to color-octet exchange, and therefore the excess above this number is attributed to color-singlet exchange. A more accurate number for this excess is obtained by making a parabolic fit to the asymmetry excluding the first two bins, extrapolating the fit to the first bin (zero tracks), subtracting the extrapolated asymmetry from the data asymmetry of the first bin, and multiplying the result by the sum of the same-side and opposite-side events in the first bin. This procedure gives consistent results even when the rapidity region of the same-side distribution is changed so that the mean values of the same-side and opposite-side distributions do not match. Using this method, we find the fractional excess over all events to be $R_1 = [2.06 \pm 0.22(\text{stat}) \pm 0.09(\text{syst})]\%$, where the systematic error reflects the uncertainty due to background subtraction and the subscript “1” refers to the $N_{\text{vertex}} \leq 1$ requirement.

The $N_{\text{vertex}} \leq 1$ selection cut, which is used to reject events due to multiple interactions, also rejects single interaction dijet events with more than one reconstructed vertex. Extra vertices in a dijet event are due to confusion in reconstruction caused by the high particle multiplicity. The ratio R_1 must therefore be corrected for the efficiency (fraction of events retained) of this cut, which affects primarily the “nongap” events, which have higher multiplicity in the central region. The efficiency for nongap events was measured to be $0.55 \pm 0.05(\text{syst})$ by comparing the fraction of single vertex dijet events to all dijet events in a given run with the fraction expected from the instantaneous luminosity in the same time period. The assigned uncertainty is due to the variations found as a function of instantaneous luminosity. For “gap” events, the vertex selection efficiency was found to be $1.00^{+0.00}_{-0.03}$. Correcting R_1 for the vertex selection efficiency we obtain for the color-singlet fraction the value

$$R = [1.13 \pm 0.12(\text{stat}) \pm 0.11(\text{syst})]\%.$$

This result is in good agreement with the published results of CDF [4] and D0 [5] and, as stated previously, its magnitude indicates that the dijet system is produced by strongly interacting color-singlet exchange.

A similar analysis was performed using the multiplicity of calorimeter towers with measured $E_T > 200$ MeV within $|\eta| < 1.0$ for opposite-side and $|\eta| < 1.25$ for same-side events. In Figs. 2(b) and 2(d), a clear excess is seen in opposite-side over same-side events in the bins $N_{\text{tower}} = 0, 1$, and 2. The combined excess in these three bins yields a fraction of $[1.92 \pm 0.20(\text{stat})]\%$;

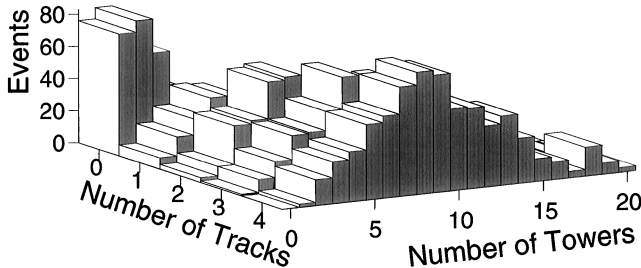


FIG. 3. Track versus tower multiplicity distribution for events in the $N_{\text{vertex}} < 1$ opposite-side dijet sample with $N_{\text{track}} < 5$ and $N_{\text{tower}} < 21$ within $|\eta| < 1.0$. The bins with zero tracks and 0, 1, or 2 towers contain an excess of events above the expectation from an extrapolation from the bins with $N_{\text{track}} > 1$. This excess is attributed to events from color-singlet exchange.

incorporating the fourth bin yields $[2.21 \pm 0.25(\text{stat})]\%$. These values are consistent with the result obtained from the track multiplicity analysis. The spilling of the rapidity gap signal into nonzero tower-multiplicity bins is mainly due to calorimeter noise, with some additional spreading resulting presumably from γ 's entering the gap region from the decay of parent neutral mesons produced within the jet regions. Because of the larger systematic uncertainties involved in the tower multiplicity analysis, we used above only the tracking result, R_1 , in deriving the color-singlet fraction R .

Figure 3 shows the correlation of towers versus tracks for opposite-side dijet events with $N_{\text{track}} < 5$ and $N_{\text{tower}} < 21$ within $|\eta| < 1.0$. The bins with $N_{\text{track}} = 0$ and $N_{\text{tower}} = 0, 1$, or 2, in which the color-singlet exchange signal is expected to be concentrated, contain a total of 221 gap events. From an analysis of the results obtained from the tracking and tower multiplicities (Fig. 2), we estimate that these 221 events contain about 15% color-octet exchange background. For this reason, and as a check for possible detector biases, we present distributions of kinematical variables of the gap events along with corresponding distributions of a control sample consisting of events with 1, 2, or 3 tracks and up to 6 towers. Figure 4 shows normalized ratios of gap and control sample events to all events as a function of the average E_T of the two leading jets, the E_T of the third jet, and the η separation of the two leading jets. In each case, the total number of gap or control sample events is normalized to the number of “all events.” The gap and control samples behave similarly. The colorless exchange fraction is fairly independent of jet E_T and $\Delta\eta$, decreasing somewhat at large $\Delta\eta$.

In the two-gluon model of Ref. [2], the gap to non-gap ratio is predicted to be independent of jet E_T and $\Delta\eta$. Calculations [9] using a model [10] based on the Balitsky-Fadin-Kuraev-Lipatov (BFKL) [11] resummation of a color-singlet gluon ladder exchange also predict a “basically flat” [12] distribution of R versus $\Delta\eta$. Our results are in general agreement with these predictions, but fur-

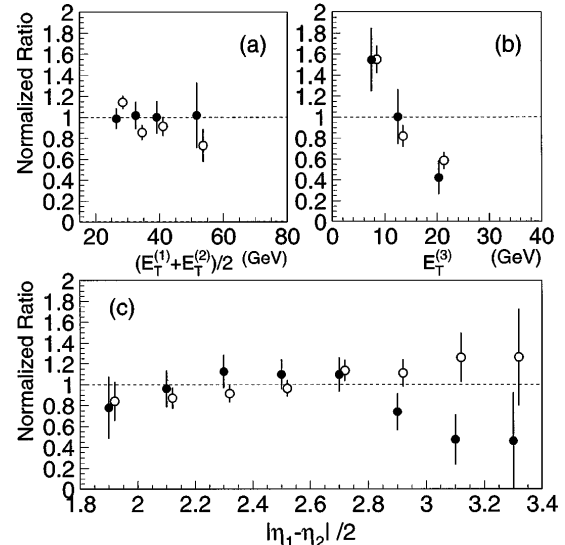


FIG. 4. Normalized (to be unity on average) ratios of gap (solid points) and control sample events (open circles) over all events versus: (a) the average E_T of the two leading jets, (b) the E_T of the third jet, and (c) half the η separation between the two leading jets.

ther investigations with higher statistics are needed before firm conclusions can be drawn about the nature of the color-singlet exchange process.

In conclusion, we report a new measurement of the fraction of dijet events with a rapidity gap between jets in $p\bar{p}$ collisions at $\sqrt{s} = 1.8$ TeV and present the results of a study of rapidity-gap event characteristics. We find that for jets of $E_T^{\text{jet}} > 20$ GeV, pseudorapidity $1.8 < |\eta| < 3.5$ and $\eta_1\eta_2 < 0$, the fraction of events that can be attributed to color-singlet exchange is $[1.13 \pm 0.12(\text{stat}) \pm 0.11(\text{syst})]\%$, in good agreement with previous measurements [4,5]. The rapidity-gap fraction is fairly independent of jet E_T within $25 < E_T < 55$ GeV and of the rapidity interval between the jets within $4 < \Delta\eta < 6$, decreasing somewhat at the largest values of $\Delta\eta$.

We thank the Fermilab staff and the technical staffs of the participating institutions for their vital contributions. This work was supported by the U.S. Department of Energy and National Science Foundation; the Italian Istituto Nazionale di Fisica Nucleare; the Ministry of Education, Science and Culture of Japan; the Natural Sciences and Engineering Research Council of Canada; the National Science Council of the Republic of China; and the A. P. Sloan Foundation.

*Visitor.

[1] We use rapidity and pseudorapidity, η , interchangeably; $\eta = -\ln(\tan \frac{\theta}{2})$, where θ is the polar angle of a particle with respect to the proton beam direction. The azimuthal angle is denoted by ϕ , and the transverse momentum (energy) of a (particle) jet, is defined as $P_T(E_T) = P(E) \sin \theta$.

- [2] J. D. Bjorken, Phys. Rev. D **47**, 101 (1993).
- [3] H. Chehime *et al.*, Phys. Lett. B **286**, 397 (1992).
- [4] F. Abe *et al.*, Phys. Rev. Lett. **74**, 855 (1995).
- [5] S. Abachi *et al.*, Phys. Rev. Lett. **76**, 734 (1996).
- [6] M. Derrick *et al.*, Phys. Lett. B **369**, 55 (1996).
- [7] F. Abe *et al.*, Nucl. Instrum. Methods Phys. Res., Sect. A **271**, 387 (1988).
- [8] F. Abe *et al.*, Phys. Rev. Lett. **79**, 2636 (1997).
- [9] V. Del Duca and W.-K. Tang, Phys. Lett. B **312**, 225 (1993).
- [10] A. H. Mueller and W.-K. Tang, Phys. Lett. B **284**, 123 (1992).
- [11] L. N. Lipatov, Sov. J. Nucl. Phys. **23**, 338 (1976); E. A. Kuraev, L. N. Lipatov, and V. S. Fadin, Sov. Phys. JETP **44**, 443 (1976); Sov. Phys. JETP **45**, 199 (1977); Ya. Ya. Balisky and L. N. Lipatov, Sov. J. Nucl. Phys. **28**, 822 (1978).
- [12] V. Del Duca, in *Proceedings of the 10th Topical Workshop on Proton-Antiproton Collider Physics, Fermilab, 1995* (AIP, Woodbury, NY, 1996).